Transactions of the 17th International Conference on Structural Mechanics in Reactor Technology (SMiRT 17)
Prague, Czech Republic, August 17 –22, 2003

Paper # F05-3

Comparison of Crack Initiation Life Estimation Procedures under Creep-fatigue Conditions

Dr M P. O'Donnell[1)] and Dr Y Takahashi[2)]
1) British Energy, Engineering Division, Barnett Way, Barnwood, Gloucester, GL4 3RS, UK.
2) CRIEPI, Material Science Department, 2-11-1, Iwado Kita, Komae-shi, Tokyo 201-8511, Japan.

ABSTRACT

This paper describes the application of "high temperature structural integrity assessment procedures" developed in the UK and Japan to creep-fatigue crack initiation in welded Type 316 features tests. The components were subjected to both fatigue and creep-fatigue loading at 630°C. The loadings are representative of those on the upper seal gimbal joint in an Advanced Gas cooled Reactor (AGR), except that the tests were isothermal and the imposed dwell times were reduced. It is demonstrated that application of the procedures gives accurate predictions of the observed crack initiation in the weldment, based on two different advanced inelastic constitutive models (BE and CRIEPI models) and best estimate materials data. Application of simplified assessment methods based on elastic analysis is shown to be conservative. Where appropriate, contrasts between the UK and the Japanese assessment procedures and inelastic modelling techniques have been highlighted.

KEY WORDS: Creep-fatigue, crack initiation, assessment procedures.

INTRODUCTION

Assessment of the integrity of structures operating at high temperature under creep-fatigue type loading conditions is of key importance for the safe and reliable operation of both nuclear and conventional power generation plant. The requirement to regularly assess the integrity of generating plant has led to the development of the R5 procedures [1] within the UK. R5 provides comprehensive advice on the assessment of both defect-free and defective structures operating at high temperatures within the creep range. For the assessment of the integrity of defect-free components, R5 assessments can be performed by either using simplified methods based on elastic analyses or by performing inelastic analyses. For the assessment of defect free components the following mechanisms are considered; excessive plastic deformation; creep deformation and rupture; creep enhanced by cyclic loading; and, combined creep-fatigue damage. In Japan, significant work has led to the development of a structural integrity guideline [2] for the assessment of Fast Breeder Reactor (FBR) plant. This guideline is based on developments for long term integrity assessments using inelastic analysis techniques and creep-fatigue life estimation methods, which are similar to those used in R5. Further, advanced constitutive models have been developed in the UK and Japan to enable inelastic analyses to be performed for components subjected to cyclic inelastic loading with creep stress relaxation during dwell periods. In the UK, the fast reactor state variable model [3, 4] (BE model) has been developed to model the behaviour of both ferritic and austenitic steels, while in Japan a constitutive model has been developed by the Central Research Institute of Electricity Power Industry (CRIEPI model) [5, 6] for a specific Type 316 steel developed for use in FBR plant.

TEST PROGRAMME AND EXPERIMENTAL RESULTS

The experimental configuration and the applied loading conditions during the test are shown in Fig. 1(a). A new upper seal gimbal joint made from Type 316 stainless steel was used to manufacture the feature test samples. Type 316 weld metal was used for the weldment; its location is shown in Fig. 1(b). Fatigue and creep-fatigue tests were conducted at a temperature of 630°C under displacement controlled conditions. The imposed displacement of ±0.25 mm, see Fig. 1(b), results in a strain range at the weld cap which is representative of the component under reactor conditions. Three tests were conducted; a fatigue test and two creep-fatigue tests, with dwell periods of 1 and 6 hours, respectively. The dwell period was imposed such that the critical region in the weld cap, see Fig. 1(b), was subjected to tensile stress during the hold time. The tests were terminated when the peak load reduced by 20% of the plateau value (similar to standard fatigue endurance tests). The test components were then sectioned for microscopic examination, see Fig. 2(a) to (c). These figures include the observed number of cycles, N, up to test termination and the corresponding crack initiation depths, a_o, in the weld cap region. It can be observed that the number of cycles decreases with the introduction of a creep dwell. For Test T1, the pure fatigue test, a fatigue crack was observed to have initiated at the weld cap (a_o=0.156mm), see Fig. 2(a). For the creep-fatigue tests, very small defects of approximately 0.015 mm and 0.025 mm depth were observed for the 1 and 6 hour dwell period tests, respectively, see Figs 2(b) and (c).

For the component assessed, there were two locations of interest for structural integrity; the weld cap, for crack initiation as noted above; and the unfused land, for crack growth. For brevity, this paper focuses on creep-fatigue crack initiation at the weld cap only, and details of the assessment of the unfused land have not been included.

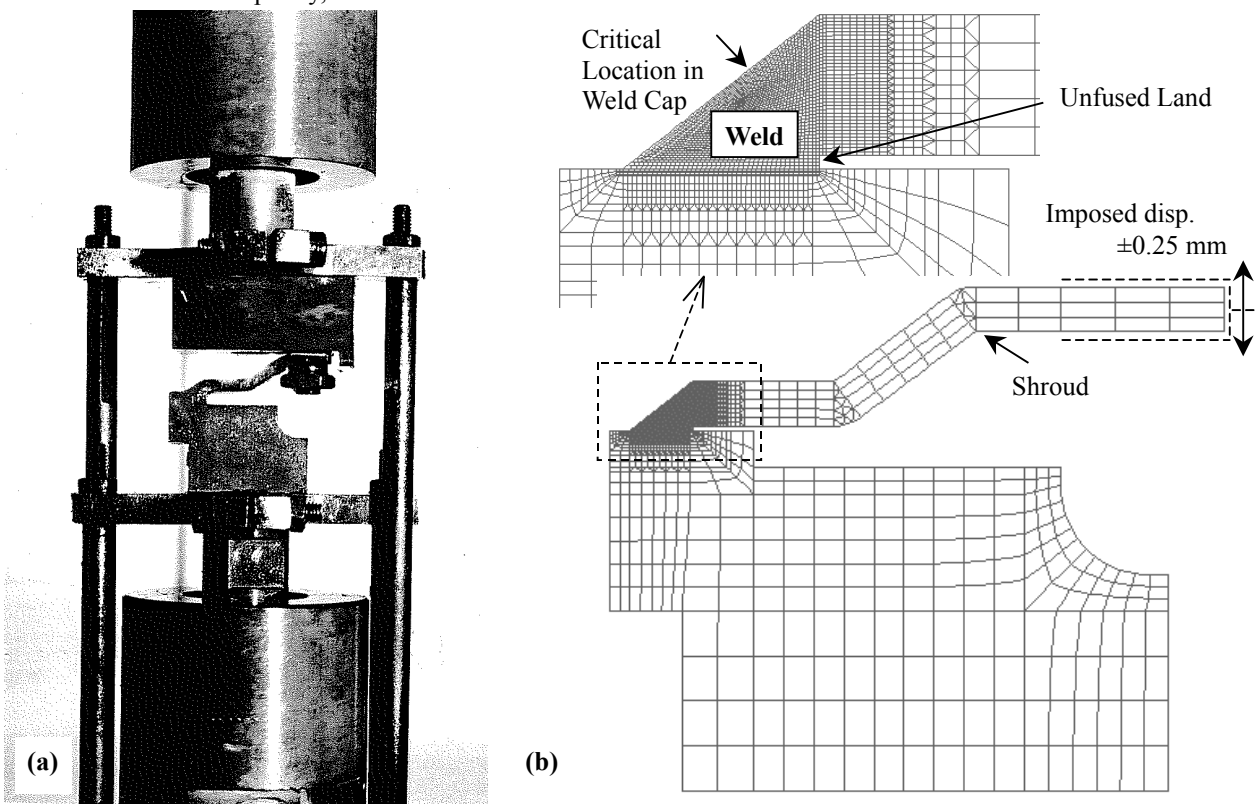

Fig. 1 Upper seal gimbal features test (a) Experimental set-up (b) Finite element (FE) model

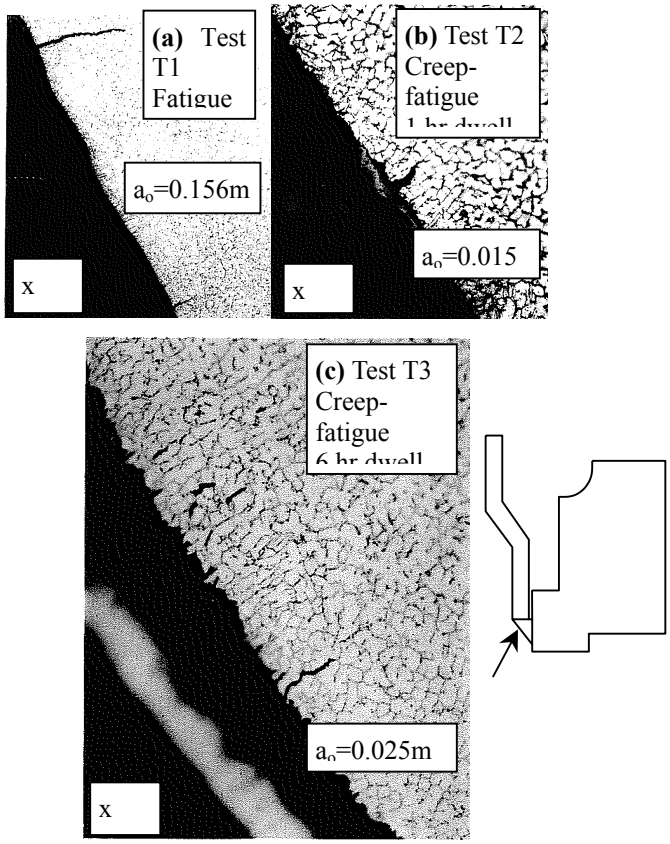

Fig. 2 Optical micrographs for crack initiation at the weld cap (a) T1, (b) T2, and (c) T3

MATERIAL PROPERTIES

Stress-strain properties

The stress verses plastic strain relations for both monotonic and cyclic loading are shown in Fig. 3. Data for the parent and weld materials have been included along with tensile properties from the BE materials data handbook, R66 [7]. The following three points are of note: first, it is clear that the parent material hardens significantly with cycling; secondly, the weld material shows some softening at strain ranges just beyond yield but the overall variation with cycling is small; finally, it can be seen that the saturated parent properties provide a conservative approximation of the weld material when used to estimate start-of-dwell stress for creep damage calculations. For the inelastic models used in the finite element (FE) calculations, there were insufficient data to determine the weld material parameters. Hence, saturated parent material properties are used to represent the weld. The effect of this assumption is discussed later.

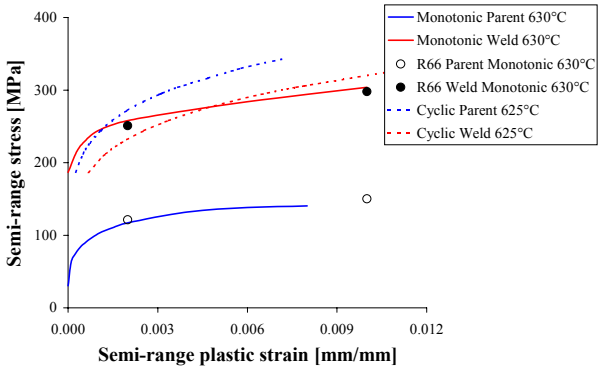

Fig. 3 Monotonic and cyclic stress-strain curves

Fatigue endurance

The following expression was used to calculate the fatigue endurance, N_ℓ, for the weld metal at 630°C [8]:

$$\Delta\varepsilon_{total}(\%) = A\left(f(T).N_\ell\right)^{-\alpha} + C \tag{1}$$

where A=22.324, C=0.220882, α=0.44589, and $f(T)$ is a temperature dependent term with $f(T)=1$ for T≤600 °C and $\log(f(T)) = D(T-600)$ for T>600°C; D=0.0099065. It is important to note that the fatigue endurance should relate to the initiation of a crack of allowable depth, a_o, which may not be consistent with the experimental fatigue endurance, N_ℓ. An empirical method for obtaining the number of cycles to initiation, N_i, is given in R5 [1] as:

$$\ln(N_i) = \ln(N_\ell) - 8.06N_\ell^{-0.28} \tag{2}$$

The number of cycles, N_g', to grow the defect from the nucleation size, a_i=0.02 mm, to a_o is obtained assuming a growth law linear in defect size, where $N_g'=MN_g$, and $N_g = N_\ell - N_i$ and M is defined as follows:

$$M = \left(a_{min}\ln(a_o/a_{min}) + (a_{min}-a_i)\right)/\left(a_{min}\ln(a_\ell/a_{min}) + (a_{min}-a_i)\right) \quad \text{for } a_o>a_{min} \tag{3}$$

$$M = (a_o - a_i)/\left(a_{min}\ln(a_\ell/a_{min}) + (a_{min}-a_i)\right) \quad \text{for } a_o<a_{min} \tag{4}$$

a_{min} is taken to be 0.2 mm [9]. The sum N_i+N_g' gives the number of cycles, N_o, to initiate a defect of depth a_o. Similarly, the Japanese approach adopts an empirical method for estimation of fatigue initiation from fatigue endurance data. However, it differs in detail, in that the number of cycles, N_o, to initiate a surface defect, a_{os}, are given by:

$$N_o = 0.5\left(N_\ell \log(a_{os}) + 1\right) \tag{5}$$

where a_{os} is the surface crack length in millimetres. Assuming a semi-elliptical crack ratio of 10:1 the Japanese expression for Type 316FR [2] gives similar predictions at 630°C. The fatigue endurance expression given in Eq. (1) has been used in conjunction with Eqs (2)-(4) to evaluate N_o and hence fatigue damage in the current assessment.

Creep ductility

The following expression was used to calculate the creep ductility, ε_f, for the weld metal [10]:

$$\log_{10}(\varepsilon_f(\%)) = \left[a + b\log(t_r) + c\log(t_r)^2\right] \pm 0.458 \tag{6}$$

where ε_f is in percent, a=1.137, b=0.3616 and c=-0.10751 and t_r is the creep rupture time in hours. The above expression can be solved to give creep ductility as a function of the average equivalent creep strain rate, $\dot{\bar{\varepsilon}}_c$ in %/hr,

where $\dot{\bar{\varepsilon}}_c = \varepsilon_f / t_r$. Both R5 and the Japanese approach recommend a ductility exhaustion approach for the calculation of creep damage. However, R5 advocates the use of rate dependent ductility, whereas the use of rate independent ductility is consistent with recommendations in the Japanese approach; this is considered further in the discussion.

Creep rupture

Weld creep rupture times, t_r, are based on the following expression [7]:

$$\ln(t_r) = -1370.97742 + 392.017365\log(T) - 7585.32666\log(\sigma)/T + 218033.456/T - 21.1028328\sigma/T \qquad (7)$$

where T is temperature in Kelvin and σ is stress in MPa. Lower bound behaviour is given by a factor of 1.33 on stress.

Creep deformation

Parent creep deformation properties have been developed for use with both the BE model [4] and the CRIEPI model [5]. Weld creep deformation properties have been determined based on scaling the parent creep deformation. The scaling applied within the BE model corresponded to a reduction of 14 on the maximum primary creep strain level and a reduction of 2.3 on the steady state creep rate. For the CRIEPI model, the creep deformation properties of the parent were scaled by applying a factor (α_c) to the creep rupture time used within the formulation of the creep deformation expression. A value of α_c =0.03 was used in the current assessment. Both of the constitutive models employed are only applicable to primary and secondary creep deformation. A comparison of the scaled deformation response and weld material test data from constant stress creep tests at 625°C is illustrated in Fig. 4. The test data, particularly at the higher stress levels, exhibited tertiary creep behaviour, which is not considered in the creep deformation models. It can be seen that there are some differences in the predicted primary creep strain. Nevertheless, both models are considered to give a reasonable approximation of the primary-secondary creep deformation over the stress levels of interest.

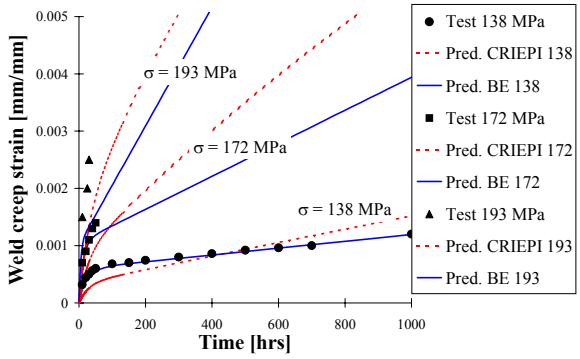

Fig. 4 Estimated Type 316 weld creep properties at 625°C

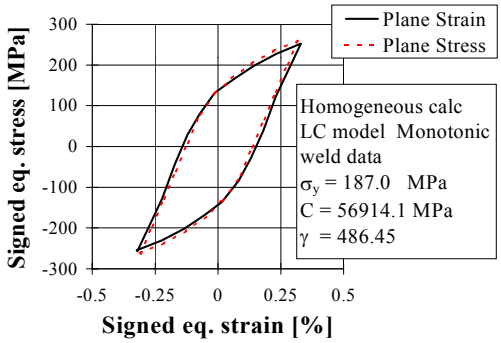

Fig 5. Comparison of plane strain and plane stress

INELASTIC FINITE ELEMENT (FE) ANALYSES

The FE model of the feature tests is shown in Fig. 1(b). The mesh consisted of 1526 triangular elements in the weldment region and 3230 quadrangular reduced integration elements for the other regions of the component. Loading was applied by constraining all of the nodes at the end of the shroud to displace between ±0.25 mm in the y-direction. The model was completely constrained at the base. The calculations were carried out using the ABAQUS FE code [11].

The recommended approach to constitutive modelling in R5 [1] (BE model) and the Japanese approach (CRIEPI model [5]) follow a similarly practical methodology, where time dependent (creep) and time independent (plastic) strains are treated separately. Complete mathematical details for the BE and the CRIEPI models can be found in [3] and [6], respectively. The BE model treats plasticity through a non-linear kinematic back stress which can isotropically harden or soften with cycling. Isotropic hardening up to cyclic saturation is determined as a linear function of the total cyclic strain energy density, given by the number of cycles times the hysteresis loop area. The CRIEPI model uses the superposition of 14 plastic back stress terms to represent the material non-linear plastic behaviour. This corresponds to a multi-linear approximation of the material stress-strain curve. Hardening or softening is modelled using a plastic hardening index surface, which is reset at the start of every reversed plastic loading cycle. For the treatment of creep strain both models adopt a strain hardening formulation. The BE model is based on a Norton type power law but with a creep back stress, which evolves up to a saturated value representing steady state creep. For displacement controlled cyclic loading, the rate of change of creep back stress is reset at the start of each creep dwell period. This enables some cyclic variation in the creep-back stress and gives a better representation of the stress relaxation behaviour during a dwell period. The CRIEPI model is based on a Blackburn type equation with three primary creep strain terms and a steady state creep term. The CRIEPI model, however, includes a creep-plasticity interaction term. The interaction resets the primary creep strain at the start of a dwell period. The condition, which must be met, is that the reversed plastic

strain should exceed the creep strain during the previous dwell period; otherwise primary creep strain is not reset. There is no specific plasticity-creep interaction term within the BE model, other than that required to give closed hysteresis loops for a cycle containing a creep dwell period [3]. This involves an adjustment of the kinematic back stress tensor in conjunction with the creep strain during the dwell period.

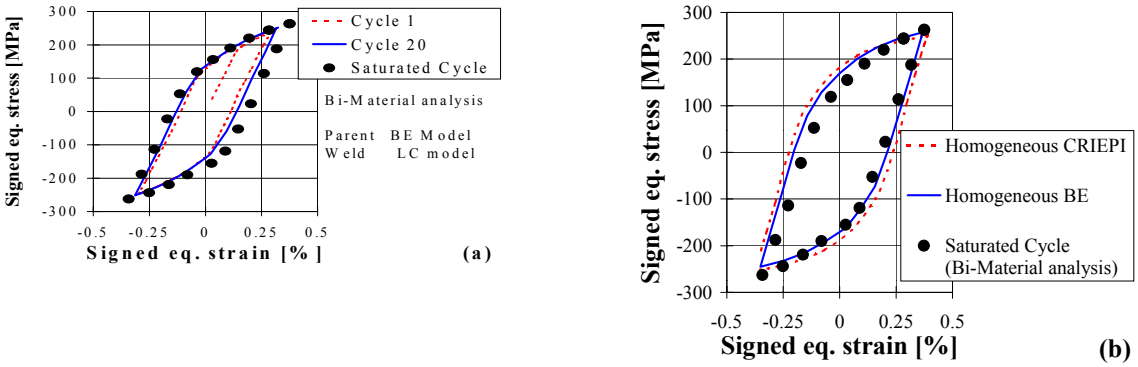

Fig. 6 Fatigue cycle at the critical location in the weld (a) Bi-material analysis and (b) Homogeneous analyses

Initially, the difference between plane stress and plane strain idealisations of the component was investigated. The non-linear kinematic model, or Lemaitre-Chaboche [12, 11] model (LC), was fitted to the monotonic weld tensile properties given in Fig. 3. The material constants used and the calculation results are shown in Fig. 5. Due to the imposed loading conditions, there is little difference between the choice of two-dimensional idealisation of plane stress or plane strain. The real structural behaviour lies between these two cases. A plane strain approximation was used in the assessment calculations. Subsequently, a set of inelastic computations were carried out in order to examine the use of saturated parent stress-strain properties to represent the weld stress-strain behaviour. The results from a bi-material analysis are shown in Fig. 6(a). The weld material properties, based on the LC model fitted to the monotonic weld stress-strain curve, were assumed not to change with cycling. The BE model was used to represent the parent material, which evolves (hardens) with cycling. It can be seen that the hysteresis loop at the critical location in the weld cap changes with hardening in the parent material; results are given for cycles 1, 20 and saturation. A comparison of the saturated fatigue cycle from the bi-material analysis with the fatigue cycle assuming saturated homogeneous parent material properties is shown in Fig. 6(b), for both the BE and CRIEPI models. In comparison to the bi-material prediction it is clear that the models used accurately represent both the peak stress in the cycle and the fatigue strain range. Finally, cyclic inelastic creep-fatigue computations were carried out using the two advanced constitutive models based on saturated parent properties. A comparison of the BE fatigue and steady state creep-fatigue cycles, given in Fig. 7(a), and those predicted by the CRIEPI model, given in Fig. 7(b), demonstrate that both models provide a similar prediction of behaviour at the critical location. However, there are some differences in detail. The CRIEPI model predicts a larger stress drop, with a correspondingly larger total strain range. This difference is derived from the fitted creep behaviour, see Fig. 4, and differences in the modelling of plasticity-creep interaction noted above.

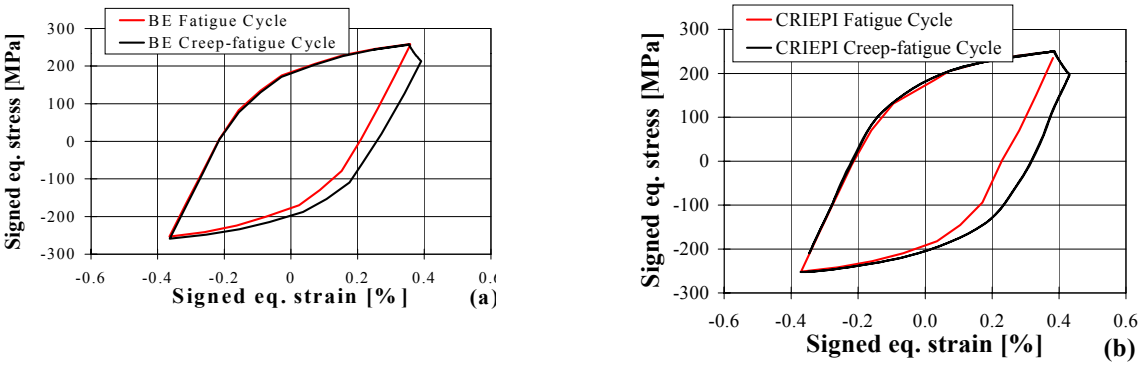

Fig. 7 Comparison of predicted fatigue creep-fatigue for (a) British Energy (BE) model and (b) CRIEPI model

ASSESSMENT OF CRACK INITIATION AT THE WELD CAP

Assessment of fatigue and creep-fatigue crack initiation at the weld cap is presented in terms of the R5 procedure [1]. Where appropriate, contrasts with the Japanese approach [5] have been highlighted.

Define the loading history: To facilitate the analysis the cyclic loading was resolved into four separate sequences as follows; (1) initial elastic-plastic loading from zero load to full load with a displacement of 0.25 mm in the shroud top; (2) creep for 0, 1 or 6 hours following initial loading; (3) unloading imposed by displacing the shroud top from +0.25 mm to -0.25 mm; and (4) reloading imposed by displacing the shroud top from -0.25 mm to +0.25 mm.

Perform elastic analysis and check margins against plastic collapse: A contour plot of the equivalent elastic stress at the end of loading is given in Fig. 8. For the weld cap the maximum value of the elastic stress range is; $\Delta\overline{\sigma}_{el,max}$ = 2 x 427.3 MPa. The margin against plastic collapse has been calculated from a limit load analysis; details are not reported. However, the FE calculations given later justify that the component will not fail by plastic collapse. They also provide justification for the required checks on the structures' ability to withstand cyclic loading.

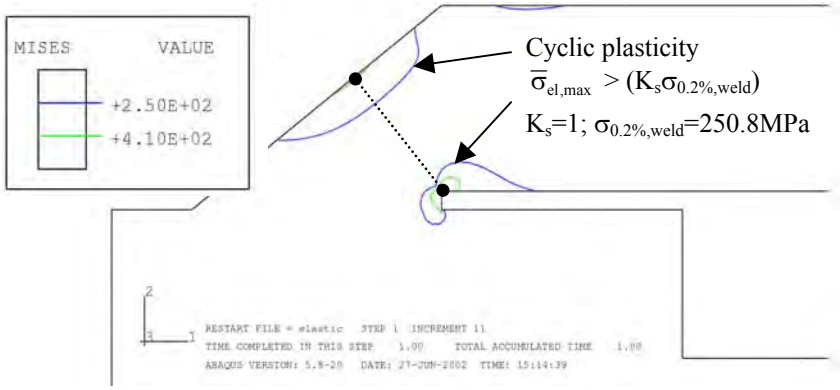

Fig. 8 Elastic equivalent stress profile local to the weldment showing regions of cyclic plasticity at the end of loading

Check margins against creep deformation and stress rupture: Excessive creep deformation and creep rupture are avoided through use of the rupture reference stress. The reference stress provides an average measure of the stress at the section of interest and needs to be adjusted for local stress concentrations as follows:

$$\chi = \overline{\sigma}_{el,max} / \sigma_{ref} \tag{8}$$

where χ is the stress concentration factor. The rupture reference stress for creep ductile material is then defined as:

$$\sigma_R = (1 + 0.13(\chi - 1))\sigma_{ref} \tag{9}$$

R5 requires the rupture reference stress to be less than the lower of the minimum rupture stress and the stress to give 1% creep strain. For the imposed loading conditions excessive creep deformation is avoided. However, creep rupture local to the weld cap may be a concern. This is consistent with the high levels of creep damage evident in Fig. 2(c).

Test for structural shakedown: The demonstration of shakedown ensures the avoidance of ratchetting. For the imposed loading, shakedown to elastic cycling cannot be demonstrated. Hence, it is necessary to consider the more relaxed global shakedown condition, where limited regions (less than 20% of a section is suggested [1]) of cyclic plasticity are permitted. Estimation of the cyclic plasticity regions local to the weld are given in Fig. 8, which shows a contour plot of the equivalent elastic stress at the maximum displacement. For isothermal and symmetric loading conditions, the cyclic regions of plasticity are given by regions where $\overline{\sigma}_{el,max} > (K_s\sigma_{0.2\%,weld})$. The material term K_s is generally less than 1.0 for softening materials, but as the magnitude of softening in the weld is small, K_s is tentatively set equal to 1.0. Also, from Fig. 8 it can be seen that just over 20% of the section was subjected to cyclic plasticity. Hence, justification of the component behaviour has been based on inelastic analysis techniques.

Define the fatigue and creep-fatigue hysteresis loops: The predicted fatigue and creep-fatigue stress-strain hysteresis loops are given in Fig. 7(a) and (b) for the BE and CRIEPI constitutive models, respectively, based on the signed equivalent stress and strain at the critical location in the weld. The simplified route in R5 and the Japanese approach, are based on elastic calculations for the estimation of the start-of-dwell stress and the creep-fatigue strain range. The results given in Figs 9(a) and (b) can be compared with the results from the detailed calculation given in Figs 7(a) and (b). For the simplified route: first, the peak stress in the cycle was estimated by projecting the maximum elastic stress range onto the weld cyclic stress strain curve. For this, R5 recommends the use of the Neuber construction. In contrast, the Japanese approach recommends a follow-up factor of 3.0; secondly, the amount of stress relaxation from the start-of-dwell stress can be calculated based on integration of the creep deformation equations [5], scaled for the weld properties. A value of Z=3.0 during creep is recommended by both approaches; thirdly, for the calculation of the creep-fatigue strain range the Japanese approach simply adds on the creep strain. In contrast, the simplified method in

R5 accounts for the effect of significant creep by increasing the maximum elastic stress range by the magnitude of the stress relaxation during the dwell. From this augmented elastic stress level an increased total creep-fatigue strain range can be calculated based on the Neuber construction, see Fig. 9(a). Finally, the total strain range needs to be corrected for the change in Poisson's ratio from elastic to plastic straining.

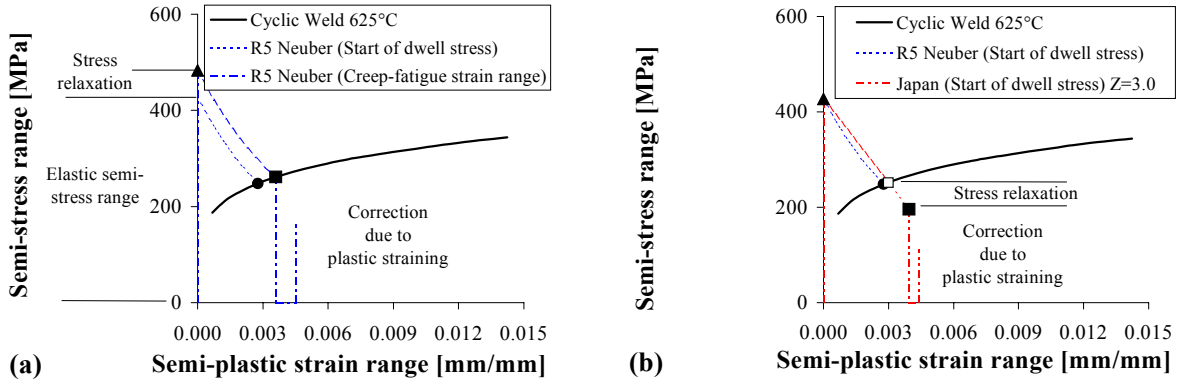

Fig. 9 Simplified approach for calculating σ_o and $\Delta\varepsilon_{total}$ (a) R5 approach (b) Japanese approach

Summarise the assessment parameters: The parameters required to calculate the creep-fatigue damage at a point can be summarised as (i) the start-of-dwell stress, σ_o, (ii) the elastic follow up factor, Z, during the dwell; and (iii) the total creep-fatigue strain range, $\Delta\varepsilon_{total}$. The parameter Z was not explicitly required in the present example as the equivalent creep strain rate occurring during the dwell was obtained directly from the FE calculations. However, Z values of approximately 2.4 and 2.2 were estimated from the BE and CRIEPI creep calculations, respectively. These can be compared with a value of Z=3.0 used in the simple elastic route recommended in R5 for isothermal structures undergoing creep stress relaxation. The same value is recommended in the Japanese approach. The key parameters can be determined from Figs 7(a) and (b) for the two different constitutive models used in the detailed assessment route.

Damage calculations: The fatigue damage per cycle, d_f, was determined as $1/N_o$, where N_o is the number of cycles to nucleate and grow a crack to a depth of a_o, determined from mean weld fatigue endurance data. It is worth noting that calculations based on lower bound fatigue endurance data, given by reducing the mean fatigue endurance by a factor of 1.33 on strain range, are conservative. Total fatigue damage was determined as $D_f=Nd_f$. The total creep damage, D_c, and creep damage per cycle, d_c, were evaluated based on the ductility exhaustion approach as follows:

$$D_c = Nd_c = N\int_0^{t_h} \dot{\varepsilon}/\varepsilon_f\left(\dot{\varepsilon}\right)dt \qquad (10)$$

where t_h is the hold time. For the detailed calculations the creep damage was evaluated directly from the FE calculations. In contrast, the simple route here used constant rate independent ductility. Having evaluated total fatigue and creep damage (D_f, D_c) separately for each test, crack initiation can be evaluated in terms of an interaction diagram, as shown in Fig. 10(a). If the assessment point (D_f, D_c) has been calculated to lie within the interaction envelope, creep-fatigue crack initiation has been avoided. Here linear damage summation is recommended. In contrast, RCC-MR [13] and N-47 [14] suggest a marginally more conservative damage envelope, which is a function of the material being assessed. However, care should be taken in comparing the different damage envelopes, as the detailed damage calculations are not the same in each case. It is clear from Fig. 10(a) that both BE and CRIEPI models give similar total damage estimates and that the simplified route is more conservative, predicting significantly more total damage.

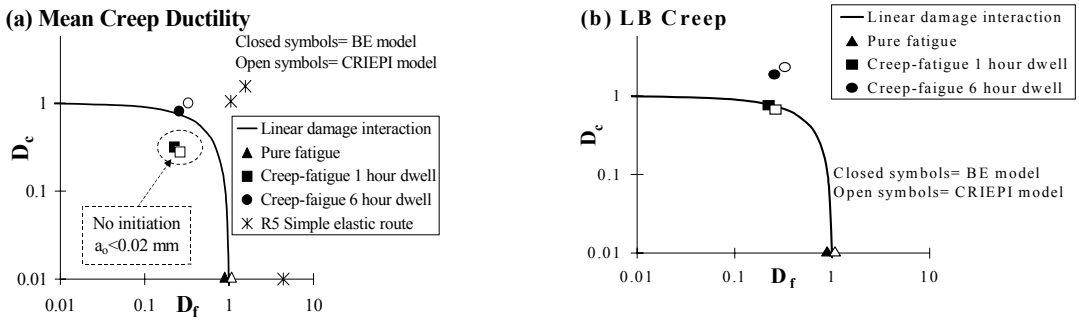

Fig. 10 Interaction diagrams for creep-fatigue evaluation (a) Mean ductility and (b) Lower bound ductility

DISCUSSION

From Fig. 10(a) it can be seen that crack initiation, defined as a_i=0.02 mm, would be conceded for both Test T1 and T3. Indeed, a defect of a_o=0.156 mm was observed for Test T1, which was taken into account in the damage assessment. For Test T3 where a_i=a_o, the assessment points confirm that the total damage was dominated by creep. For Test T2, calculated creep and fatigue damage were of a similar magnitude, and crack initiation was not predicted. The small defect which was observed for this test is smaller than but close to a_i. It should be noted that the calculations were based on mean data and due to material scatter some non-conservative results would be expected. Nevertheless, this underlines the importance of examining the sensitivity of the results to the materials data assumptions, particularly the creep ductility. It is noteworthy that the Japanese assessment approach recommends a rate independent ductility for Type 316FR material and Type 316 weld material, which is consistent with observed ductility for these materials [1, 5]. In contrast, for Type 316 stainless steel a rate dependent ductility is consistent with experimental observations [7]. The increased margin of conservatism using lower bound ductility can be seen in Fig 10(b). In the current assessment the mean rate dependent ductility data were found to be appropriate. Finally, it can be noted that for safety assessments of real plant components in general, lower bound creep ductility is used. However, for validation it is appropriate to use mean data in order to obtain a best estimate of the structural integrity of the component.

CONCLUSIONS

The high temperature structural integrity methodologies developed in the UK and Japan have been applied to a welded component, which was subjected to both fatigue and creep-fatigue loading. Crack initiation assessments based on simplified elastic techniques and full inelastic analyses have been carried out for the weld cap. It was demonstrated that accurate predictions were obtained, based on the inelastic route and best estimate materials data. Conservative predictions were obtained based on lower bound data. Application of the simplified elastic methods was shown to be conservative and the different recommendations in the UK and Japanese approaches were shown to give similar results.

ACKNOWLEDGEMENTS

This study was carried out as part of collaborative project between British Energy and CRIEPI. The work is published with the permission of both organisations. The authors would also like to thank the Royal Academy of Engineering for the provision of financial support for the collaboration through the Foresight award scheme.

REFERENCES

1 Ltd., An Assessment Procedure British Energy Generation for the High Temperature Response of Structures, R5 Issue 3, 2003.
2 Takahashi, Y., Development of Structural Integrity Assessment Guideline for FBR Components, PVP-Vol. 5, ASME Book No. H01146, pp. 209-214, 1998.
3 White, P.S., Fast Reactor State Variable Model for Cyclic Inelastic Analysis of Type 316 Stainless Steel, SMiRT Vol. L, pp. 83-88, 1993.
4 Bate S.K. and Slater I.J., Development of the Fast Reactor State Variable Model - Evaluation of Material Parameters, AEA Technology Report AEAT 3104 - PC/AGR/5086, (1998).
5 Takahashi, Y., Advancement of High Temperature Structural Design Method for Fast Reactor Components. Part I: Creep-Fatigue Damage Evaluation Method for 316FR, PVP-Vol. 5, ASME Book No. H01146, pp. 159-166, 1998.
6 Takahashi, Y., Advancement of High Temperature Structural Design Method for Fast Reactor Components. Part II: Inelastic Constitutive Model for 316FR, PVP-Vol. 5, ASME Book No. H01146, pp. 167-174, 1998.
7 Hamm, C.D. (Ed.), AGR Materials Data Handbook, R66, Issue 5, British Energy Generation Ltd., 1999.
8 Sore, R.P., Fatigue Endurance of Austenitic Stainless Steels and Weld Metals, British Energy Generation Report E/REP/AGR/0161/00, 2001
9 Pineau, A., High Temperature Fatigue Behaviour of Engineering Materials in Relation to Microstructure, in Fatigue at High Temperature, ed. R P Skelton, Applied Science, London, 305-364, 1983.
10 Fast Reactor Data Sheet, Stress Rupture Strength and Ductility Properties of Type 17Cr-8Ni-2Mo Weld Metal for The Type 310 Stainless Steel, CEGB Report RD/L/2449/R83.
11 ABAQUS, Version 5.8, Hibbit, Karlsson and Sorensen, Inc 1994.
12 Lemaitre, J. and Chaboche, J.L., Mechanics of Solids and Materials, Cambridge University Press, ISBN 0 521 47758 1, 1990.
13 RCC-MR, Design and Construction Rules for Mechanical Components of FBR Nuclear Islands, ACFEN, 1985.
14 Cases of ASME Boiler and Pressure Vessel Code, Case N47-29 Class 1 Components in Elevated Temperature Service, Section III, Division 1, ASME, New York, 2001.